EPJ Web of Conferences **376**, 01002 (2026) https://doi.org/10.1051/epjconf/202637601002
ICRAMEN 2026

Numerical study of the center of gravity in the strengthening zone of steel with corrosion

Antonio Shopov*

Academy of Ministry of Interior, Fundamental and General Engineering Sciences, Department, 1000 Sofia City, Bulgaria

Abstract. In this paper, an unusual approach is used. The method of statistical mathematics is applied to determine the center of gravity in the strengthening zone in the stress-strain curve. The change of the center of gravity is numerically studied, and this part of the stress-strain diagram is represented as a function, respectively, it is divided into known figures, from which the center of gravity can be determined. Experimental measurements from corroded steel are utilized, and mathematical analysis is performed employing stochastic, average, and RMS techniques. Finally, the obtained results are presented, and it is noted that they also confirm that corrosion affects only strain and not stress on steel.

1 Introduction

There is almost no research [1] on the change of the center of gravity in a given function. This is considered a mathematical problem, which is more of a theoretical calculation without practical meaning, although statistical mathematics gives a clear answer to what this value would be, if it were found. According to statistical mathematics - the probability that the random variable "X" falls within a given interval is numerically equal to the area between the probability density graph in that interval and the horizontal axis i.e. formula 1 [2-5].

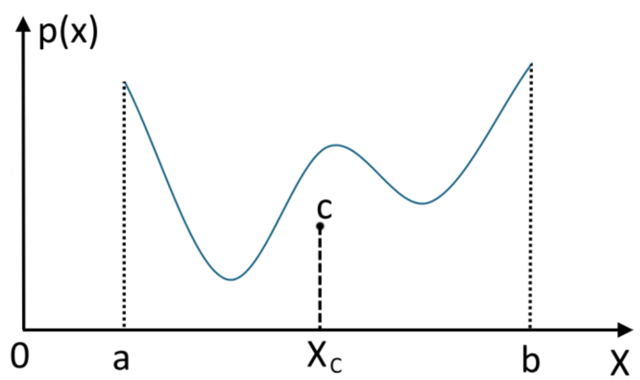

Fig. 1. Visualizing the center of gravity on the function p(x).

* Corresponding Author: shopoff@mail.bg

$$\int_{a}^{b} p(x)dx = 1 \tag{1}$$

Considering formula (For.1), it turns out that this area is equal to 1, it follows that "X" is gives the abscissa of the center of gravity of the area (Fig.1) composed of the function p(x), and it will coincide with the so-called mode (statistics) only in the presence of symmetry in the graph of the function. Consequently, should a diagram stem from a particular investigation (to make it straightforward, let's consider a planar, two-dimensional representation with just a horizontal and a vertical axis), this investigation is then depicted as a curve, illustrating a relationship. Within the X-Y axis framework, this inherently implies the presence of a shape, or more accurately termed, a "planar lamina" devoid of thickness or substance. In this case, according to mathematics, there will be a center of gravity of the figure, which can be determined by the known formula 2 [2-5]:

$$X_c = \frac{\sum_{i=1}^{n} x_i . A_i}{\sum_{i=1}^{n} A_i} \quad ; \quad p(x)_c = \frac{\sum_{i=1}^{n} p(x)_i . A_i}{\sum_{i=1}^{n} A_i} \tag{2}$$

In case this center of gravity exists (it falls inside the diagram) in, then its variation depending on the available experimental information will better explain the occurring changes or will give us the opportunity for verification of the study data, clearly delineating the boundaries of possible deviations and numerical changes.

2 Numerical method

Finding the equation of the function is practically impossible, since in this case we are using experimental data. They are, by their nature, randomly distributed values that form the curve (diagram). Given this, a principle is used in which the curve (diagram) is divided into small sections. For the shapes of which we can determine the center of gravity (since these are classical shapes — rectangle and quarter part of ellipse) and, using formulas for composite shapes, we determine the center of gravity in the selected section of the function, in this case the strengthening zone – figure 2. So that this whole zone can be calculated, by the division into infinitely small sectors, which will be composed of a rectangle and a quarter part of ellipse, this method is with sufficient accuracy for practice.

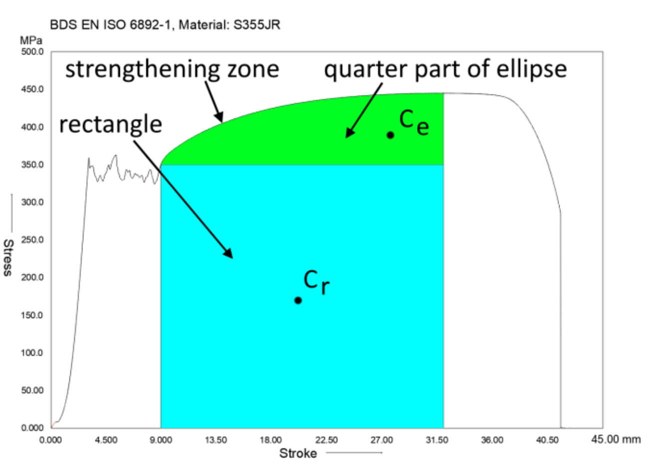

Fig. 2. Strengthening zone - one rectangle and quarter part of ellipse.

Standardly, the dimensions of the coordinates of the center of gravity are in mm, cm, etc., but since along X-axis is the deformation, which is in mm, and along Y-axis are the stresses, which are in MPa, it follows that there will be a different dimension than the expected one (Fig. 3).

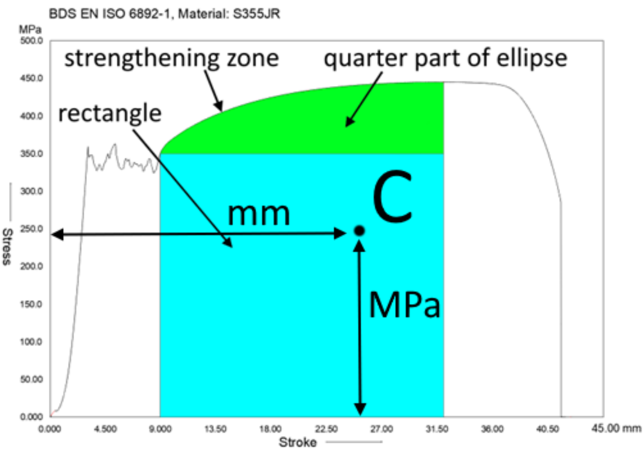

Fig. 3. Dimensions of the center of gravity.

In this approach, first the center of gravity is determined in the strengthening zone of non-corroded steel, and subsequently we determine the center of gravity of the known experimental data of corroded steel. In [6-12] sufficient experimental data have been published (fig. 4). Because these are experimental data and they are processed using well-known mathematical models - stochastic, average and root mean square (RMS).

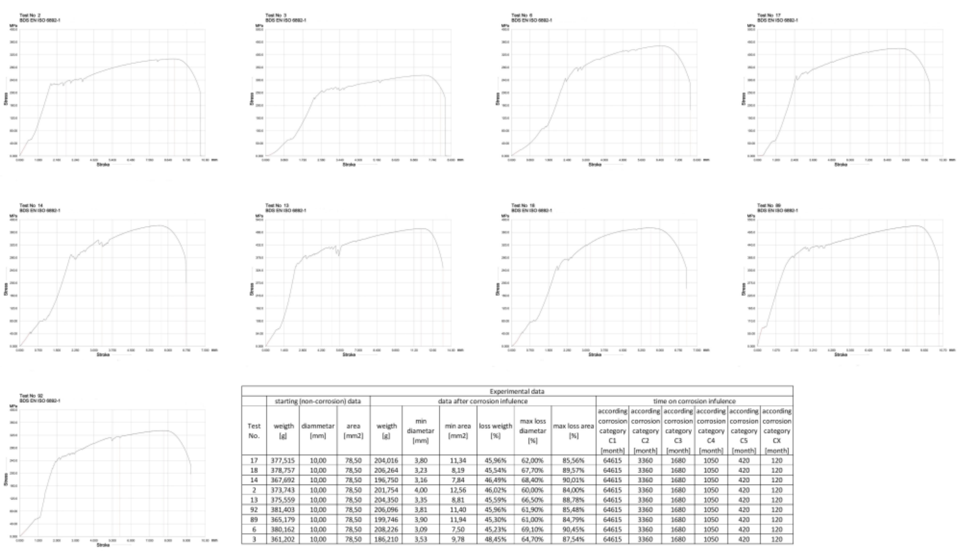

Experimental data																
	starting (non-corrosion) data			data after corrosion infulence						time on corrosion infulence					
Test No.	weigth [g]	diammetar [mm]	area [mm2]	weigth [g]	min diametar [mm]	min area [mm2]	loss weigth [%]	max loss diametar [%]	max loss area [%]	according corrosion category C1 [month]	according corrosion category C2 [month]	according corrosion category C3 [month]	according corrosion category C4 [month]	according corrosion category C5 [month]	according corrosion category CX [month]
17	377,515	10,00	78,50	204,016	3,80	11,34	45,96%	62,00%	85,56%	64615	3360	1680	1050	420	120
18	378,757	10,00	78,50	206,264	3,23	8,19	45,54%	67,70%	89,57%	64615	3360	1680	1050	420	120
14	367,692	10,00	78,50	196,750	3,16	7,84	46,49%	68,40%	90,01%	64615	3360	1680	1050	420	120
2	373,743	10,00	78,50	201,754	4,00	12,56	46,02%	60,00%	84,00%	64615	3360	1680	1050	420	120
13	375,559	10,00	78,50	204,350	3,35	8,81	45,59%	66,50%	88,78%	64615	3360	1680	1050	420	120
92	381,403	10,00	78,50	206,096	3,81	11,40	45,96%	61,90%	85,48%	64615	3360	1680	1050	420	120
89	365,179	10,00	78,50	199,746	3,90	11,94	45,30%	61,00%	84,79%	64615	3360	1680	1050	420	120
6	380,162	10,00	78,50	208,226	3,09	7,50	45,23%	69,10%	90,45%	64615	3360	1680	1050	420	120
3	361,202	10,00	78,50	186,210	3,53	9,78	48,45%	64,70%	87,54%	64615	3360	1680	1050	420	120

Fig. 4. Graphics of the experimental data are used [11].

3 Numerical study

According to standard ISO 9223, we have six corrosion categories, which essentially differ only in the rate of corrosion development over time, and are accepted as different variants.

3.1 Steel without corrosion

These are the initial data, which due to the corrosion influence change depending on time. The basic obtained calculation result is given in table 1.

Table 1. Calculation results on steel without corrosion.

Coordinates	Stochastic result	Average result	Root mean square result
ε_c , [mm]	18,9684534	19,56262931	19,58820045
σ_c , [MPa]	214,9127044	213,5218679	213,5461496

3.2 Corrosion variant A

Variant A corresponds to corrosion influence, for corrosion category C1 - 9139 months; C2 - 475 months; C3 - 238 months; C4 - 149 months; C5 - 59 months and CX - 17 months. The obtained calculation result is given in table 2.

Table 2. Calculation results on corrosion variant A.

Coordinates	Stochastic result	Average result	Root mean square result
ε_c , [mm]	19,02384744	16,0992279	17,98701383
σ_c , [MPa]	210,0212478	206,3073544	207,6507272

3.3 Corrosion variant B

Variant B consists corroded steel test specimens with a diameter ranging from 8.00 to 9.00 mm according to experimental data. The application of the ISO 9223 standard gives grounds to establish that variant B corresponds to corrosion influence, for corrosion category C1 - 14769 months; C2 - 768 months; C3 - 384 months; C4 - 240 months; C5 - 96 months and CX - 28 months. The obtained calculation result is given in table 3.

Table 3. Calculation results on corrosion variant B.

Coordinates	Stochastic result	Average result	Root mean square result
ε_c , [mm]	17,08482871	16,8228484	16,93245434
σ_c , [MPa]	212,1886164	209,7358854	209,9509642

3.4 Corrosion variant C

Variant C consists of corroded steel test specimens with a diameter ranging from 7.00 to 8.00 after according to experimental data. The application of the ISO 9223 standard gives reason to establish that variant C corresponds to corrosion influence, for corrosion category C1 - 24923 months; C2 - 1296 months; C3 - 648 months; C4 - 405 months; C5 - 162 months and CX - 46 months. The obtained calculation result is given in table 4.

Table 4. Calculation results on corrosion variant C.

Coordinates	Stochastic result	Average result	Root mean square result
ε_c , [mm]	14,54874965	14,4334322	14,70750777
σ_c , [MPa]	224,976919	211,4272048	212,9199877

3.5 Corrosion variant D

Variant D consists of corroded steel test specimens with a diameter of 6.00 to 7.00 mm. The corrosion influence corresponds as follows: for corrosion category C1 - 34892 months; C2 - 1814 months; C3 - 907 months; C4 - 567 months; C5 - 227 months and CX - 65 months. The obtained calculation result is given in table 5.

Table 5. Calculation results on corrosion variant D.

Coordinates	Stochastic result	Average result	Root mean square result
ε_c , [mm]	10,51971	8,851883	9,99219
σ_c , [MPa]	210,7138	199,0996	210,3399

3.6 Corrosion variant E

The application of the ISO 9223 standard gives reason to establish that variant E corresponds to corrosion influence, for corrosion category C1 - 46154 months; C2 - 2400 months; C3 - 1200 months; C4 - 750 months; C5 - 300 months and CX - 86 months. The obtained calculation result is given in table 6.

Table 6. Calculation results on corrosion variant E.

Coordinates	Stochastic result	Average result	Root mean square result
ε_c , [mm]	9,697957	9,004804	9,488448
σ_c , [MPa]	214,8491	203,4095	204,2975

3.7 Corrosion variant F

The application of the ISO 9223 standard gives grounds to establish that variant F corresponds to corrosion influence as follows, for corrosion category C1 - 54000 months; C2 - 2808 months; C3 - 1404 months; C4 - 878 months; C5 - 351 months and CX - 100 months. The obtained calculation result is given in table 7.

Table 7. Calculation results on corrosion variant F.

Coordinates	Stochastic result	Average result	Root mean square result
ε_c , [mm]	8,459729	8,753552	8,945769
σ_c , [MPa]	217,4623	209,7418	211,9799

3.8 Corrosion variant G

In variant G the duration of the corrosive influence corresponds to the relevant corrosion category C1 - 64615 months; C2 - 3360 months; C3 - 1680 months; C4 - 1050 months; C5 - 420 months and CX - 120 months. The obtained calculation result is given in table 8.

Table 8. Calculation results on corrosion variant G.

Coordinates	Stochastic result	Average result	Root mean square result
ε_c , [mm]	6,742827	6,609094	6,879724
σ_c , [MPa]	190,1866	182,5385	185,9603

3.9 Corrosion variant H

The application of the ISO 9223 standard gives reason to establish that variant H corresponds to corrosion influence as follows: corrosion category C1 - 73107 months; C2 - 3801 months; C3 - 1901 months; C4 - 1188 months; C5 - 475 months and CX - 136 months. The obtained calculation result is given in table 9.

Table 9. Calculation results on corrosion variant H.

Coordinates	Stochastic result	Average result	Root mean square result
ε_c , [mm]	4,388576	3,503584	3,522872
σ_c , [MPa]	206,281	167,1862	170,9705

3.10 Corrosion variant I

The use of ISO 9223 standard gives grounds to establish that variant I responds to corrosion influence as follows: C1 - 77262 months; C2 - 4018 months; C3 - 2009 months; C4 - 1256 months; C5 - 502 months and CX - 143 months. The obtained calculation result is given in table 10.

Table 10. Calculation results on corrosion variant I.

Coordinates	Stochastic result	Average result	Root mean square result
ε_c , [mm]	2,868159	2,86634	2,910011
σ_c , [MPa]	209,4974	196,902	198,5927

4 Results and discussion

The comparison of the numerical results obtained is given in figure 5 and figure 6.

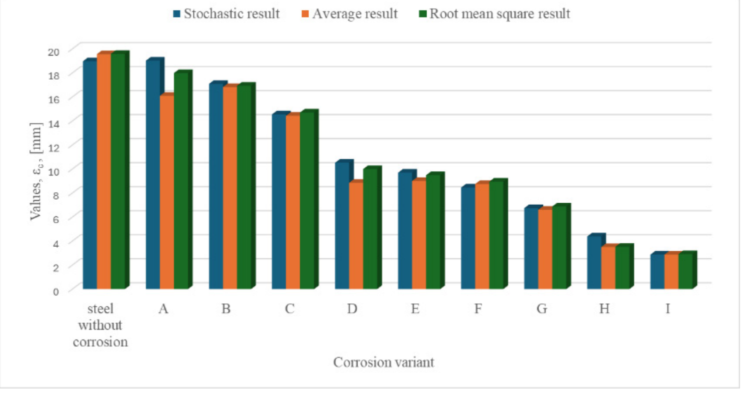

Fig. 5. Chart of the results – change on coordinates of ε_c , according to corrosion variant.

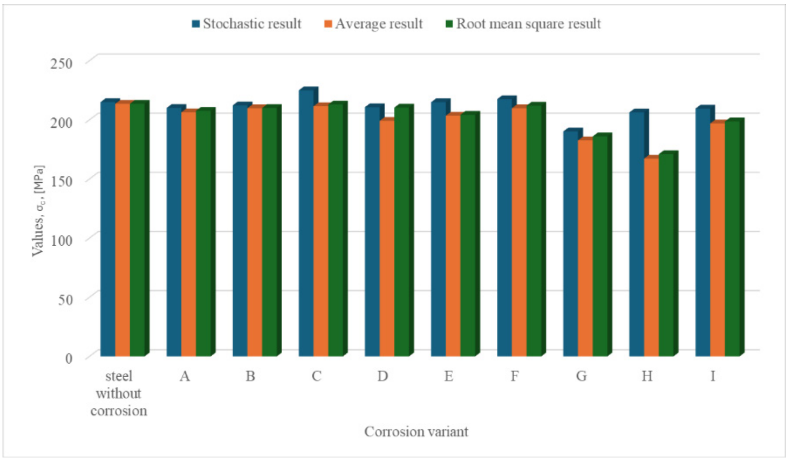

Fig. 6. Chart of the results – change on coordinates of σ_c , according to corrosion variant.

The present computational study establishes that with the onset of the corrosion effect, the degradation of the material (its transition from ductile to brittle) begins to slowly creep, in this case a decrease in the strain center of gravity is established within 9% - 14% of the initial known values. With the continued development of the corrosion effect, enhanced degradation processes begin to occur, with values reporting differences within 23% - 26% of the initial ones. Next, the degradation of ductility intensifies and in a very short time reaches values of 44% - 54%, i.e. the plasticity of the material has already decreased by 50%. The continuing corrosion effect increases the brittleness of the material and at a certain point value of 64% - 66% are reached, which is a clear sign that the material is no longer elastic, but has almost become brittle. In the last phase, values of 76% - 85% are reached, which means that the material has already lost its elasticity and has completely turned into a brittle material. Regarding the stress center of gravity, a very slow smooth decrease is observed, initially varying between 1.2% - 1.8%, which can be considered almost non-existent, and subsequently reaching the highest values which vary between 14.5% - 21.7%, i.e. we can safely assume that corrosion does not have any effect on the expected value of the strength of the material.

5 Conclusion

Numerical study of the strengthening zone just like a function, a change in the center of gravity was found, especially in the X-axis. As a result, it reached 85%, i.e. almost before the general change, namely the transformation of steel from ductile to brittle material. Which confirms the fact that corrosion affects only and only the ability of ductility, and not the strength properties of steel. On the other hand, strain is a basic parameter of ductility and its reduction unambiguously defines that in the late phase of the impact of corrosion the only thing that will happen is a loss of bearing capacity due to excessive deformations. On the other hand, the present study proved that it is possible to apply the methods of mathematical statistics and through them to confirm or reject the relevant possible assumptions, i.e. they can be used as verification for the results obtained.

References

1. S. Mukherjee, Locating center of gravity in geological contexts. Int. J. Earth Sci. (Geol. Rundsch.) 107, 1935–1939 (2018). https://doi.org/10.1007/s00531-017-1560-z
2. S. Kislyakov, Stokhastichni metodi v prilozhnata mehanika (Tekhnika, Sofia, 1981) (in Bulgarian)
3. B. Bagchi, Statistical mechanics for chemistry and materials science (CRC Press, Boca Raton, 2019)
4. R.C. Tolman, The principles of statistical mechanics (Courier Corporation, North Chelmsford, 1979)
5. M. Spiegel, S. Lipschutz, J. Liu, Schaum's outline of mathematical handbook of formulas and tables (McGraw-Hill Education, Columbus, 2017)
6. F. Tariq, P. Bhargavaz, Stress–strain curves and mechanical properties of corrosion damaged super ductile reinforcing steel. Structures 33 (2021). https://doi.org/10.1016/j.istruc.2021.05.039
7. N. Zhao, C. Zhang, Experimental investigation of the mechanical behavior of corroded Q345 and Q420 structural steels. Buildings 13(2), 475 (2023). https://doi.org/10.3390/buildings13020475
8. C. Jeon, J. Lee, S. Lon, C. Shim, Equivalent material model of corroded prestressing steel strand. J. Mater. Res. Technol. 8 (2019). https://doi.org/10.1016/j.jmrt.2019.02.010
9. D. Makedonska, V. Tsanov, Development of experimental equipment for testing fire extinguishing nozzles in underground mining sites. EPSTEM 35 (2025). https://doi.org/10.55549/epstem.1804522
10. P.S. Rao, R.H. Gajghat, V.N. Kalbande, M.A. Kumbhalkar, K.S. Rambhad, Optimization of fluidity and mechanical properties of the sand casting A518 alloy by using grey relational analysis method. AIP Conf. Proc. 2839 (2023). https://doi.org/10.1063/5.0167643
11. A. Shopov, Polinomialni funktsii za opredelqne na tendentsiyata v mechanicnite svoistva na stomanata v zavisimost ot vremeto na korozionno vliyanie (AMVR, Sofia, 2025). https://doi.org/10.5281/zenodo.15603728 (in Bulgarian)
12. Shopov, Opredelyane na vliyanieto na koroziata varxu mehanicnite svoistva na kostrustionna stomana S355JR (AMVR, Sofia, 2025). https://doi.org/10.5281/zenodo.15716288 (in Bulgarian)